chemosensors

MDPI

Article

How Meaningful Are Minor Details in the Generation of Nanomodified Electrochemical Enzyme Biosensors? Exploring the Scenario with Sinusoidal Approaches

Md. Towhidur Rahman [1], David López-Iglesias [1], Alfonso Sierra-Padilla [1], Juan José García-Guzmán [2,*], Laura M. Cubillana-Aguilera [1,*], Dolores Bellido-Milla [1] and José María Palacios-Santander [1]

[1] Department of Analytical Chemistry, Institute of Research on Electron Microscopy and Materials (IMEYMAT), Faculty of Sciences, Campus de Excelencia Internacional del Mar (CEIMAR), University of Cadiz, Campus Universitario de Puerto Real, S/N. 11510 Puerto Real, Cadiz, Spain
[2] Instituto de Investigación e Innovación Biomédica de Cadiz (INiBICA), Hospital Universitario 'Puerta del Mar', Universidad de Cadiz, 11009 Cadiz, Spain
* Correspondence: juan.garcia@inibica.es (J.J.G.-G.); laura.cubillana@uca.es (L.M.C.-A.); Tel.: +34-956-016357 (J.J.G.-G. & L.M.C.-A.)

Abstract: In this work, a screening of Sonogel-Carbon (SNGC) electrodes modified with nanomaterials (carbon nanotubes and gold nanoparticles) and the study of their effect on the electrochemical performance of sinusoidal voltage (SV) and current (SC)-based biosensors are reported. Surface modification was achieved by drop-casting and electrodeposition methodologies. Within the strategies used, SV and SC, recently exploited procedures, were used to electrodeposit simultaneously a poly 3,4-ethylenedioxythiophene (PEDOT)-tyrosinase layer and the corresponding nanostructured material. Dopamine was selected as a benchmark analyte to evaluate the analytical performance of the different (bio)sensors obtained in terms of relevant figures of merit, such as sensitivity, limits of detection and quantitation, and accuracy, among others. A discussion about the pros and cons between the type of modification and the methods employed is also presented. Briefly, SC based sensors offered excellent quality analytical parameters and lower dispersion of the results. They were employed for more specific electrochemical studies, including interferences assays and the determination of DA in real samples, obtaining good recoveries (101–110.6%). The biosensor modified with gold nanoparticles (AuNPs) (drop-casting method) and SC-electrodeposited showed the best figures of merit: R^2 = 0.999; sensitivity = -4.92×10^{-9} A·μM^{-1}; $RSD_{sensitivity}$ = 1.60%; LOD = 5.56 μM; RSD_{LOD} = 6.10%; and LOQ = 18.53 μM.

Keywords: Sonogel-Carbon (bio)sensors; gold nanoparticles; carbon nanotubes; tyrosinase; sinusoidal methods; 3,4-ethylenedioxythiophene; dopamine

Citation: Rahman, M.T.; López-Iglesias, D.; Sierra-Padilla, A.; García-Guzmán, J.J.; Cubillana-Aguilera, L.M.; Bellido-Milla, D.; Palacios-Santander, J.M. How Meaningful Are Minor Details in the Generation of Nanomodified Electrochemical Enzyme Biosensors? Exploring the Scenario with Sinusoidal Approaches. *Chemosensors* **2022**, *10*, 316. https://doi.org/10.3390/chemosensors10080316

Academic Editors: Teresa Corrales, Nicole Jaffrezic-Renault and Eleonora Alfinito

Received: 5 July 2022
Accepted: 4 August 2022
Published: 7 August 2022

1. Introduction

Biosensors stand as a highly growing field of research nowadays. Indeed, 5313 papers concerning biosensors were published in 2021 according to Scopus database, which means almost 15 papers per day. This continuous spread is mainly due to their numerous advantages such as sensitivity, reproducibility, miniaturization capability, quick response, and online analysis, among others. In addition, the incorporation of a biological recognition element provides selectivity to the system, resulting in a high potential device. Importantly, many meaningful analytes are electroactive species including pollutants [1,2] and biomolecules for human health monitoring [3–9]. This is why electrochemical biosensors can be proposed as natural approach for their monitoring. Furthermore, the interest in these devices is not only owing to the straightforward approach, as inhibition biosensors [10,11] can also be employed to indirectly determine analytes such as heavy metals. Thus, many authors have devoted great efforts toward the development of new and more efficient

electrochemical biosensors. It is also possible to note that one possible, feasible evolution in the healthcare systems refers to the "eHealth" concept and a more decentralized system. In this scenario, a wireless portable device which allows continuous monitoring of relevant biomarkers is highly appreciated.

Nevertheless, despite of the abovementioned native advantages, biosensors are usually modified to improve their features, such as sensitivity, limit of detection, and reproducibility, or other features, e.g., fouling resistance and stability, among others. In this regard, nanomaterials and conducting polymers are two of the most representative modifiers employed for this purpose.

Since their first development in the 1970s, conducting polymers (CPs) have attracted the attention of a huge number of scientists. Within the electroanalytical field, it has been demonstrated the suitability of these polymers for sensor modification, mainly due to the possibility of performing in situ syntheses onto the surface of an electrode via electrochemistry. On the one hand, it is possible to precisely control all the parameters involved in the electrodeposition (i.e., monomer concentration, deposition time, current involved, etc.), making the process highly reproducible. It is also possible to tailor their intrinsic features: conductivity modifications can be achieved by doping process and the rheological and textural properties are susceptible to be altered with different electrochemical methodologies. On the other hand, the polaron-bipolaron mechanisms involved in the polymer growth open the door to the entrapping of several compounds inside the polymer matrix during the electrodeposition, including enzymes, making them an excellent candidate in the constitution of biosensor devices [12–14].

Alternatively, nanomaterials, especially metallic nanoparticles and carbon nanotubes, have been also frequently used to modify electrochemical biosensors. Regarding the nanoparticles, noble metal nanoparticles, such as gold nanoparticles [15–17] or platinum nanoparticles [18–20] have very desirable properties, such as high surface-to-volume ratio, high surface energy and high electrical conductivity, among others. These properties allow the nanoparticles to have a wide range of possible roles, e.g., immobilizing platforms, and perhaps most exploited in biosensors, the ability to act as electron roads to drive electrons produced from the bioreactions to the transducer in the electrode surface [21].

On the contrary, many pieces of research are focused on the employment of nanosize carbon allotropes, such as fulerenes [22], graphene [23], and carbon nanotubes (CNTs) [24], seeking to take advantage on their high electrical conductivity, and huge surface/volume ratio, among other properties. In this sense, as expected, biosensors modified with CNTs possess a very high electroactive surface, a higher conductivity, and an improvement of the electron transfer kinetics for a wide range of electroactive species as well [25]. Moreover, CNTs can be used with other modifiers to create nanocomposites which could offer great benefits [26].

Regardless of the advantages previously mentioned, it should be remarked that the nature of the modifiers employed is not the only aspect to consider, but the procedure to incorporate these modifiers in the biosensor can be a critical factor as well. Many approaches have been applied, e.g., the simple drop-casting method [27–30], the one-step electrodeposition [14] and the self-assembly monolayer procedure [13], among others.

In this work, the screening of a wide range of possibilities to generate PEDOT-tyrosinase biosensors by using sinusoidal voltage (SV) or sinusoidal current (SC) electrodeposition methods is reported. SV and SC have provided good results in previous studies [14,31–33]. However, the resulting biosensors have never been modified with nanomaterials before. The main aim of this paper is to take advantage of the tyrosinase-PEDOT electrodeposition for the one-step generation of a biosensor modified simultaneously with nanomaterials and conducting polymers and examine its output results according to the different of the approaches used. Moreover, other kinds of modifications, such as the drop-casting method, were also studied for comparison purposes. To the best of our knowledge there is no study with the same purpose in literature and even if many authors have remarked the excellent properties of their proposed device, it is not frequent the

demonstration of why the exposed methodology is better than other similar non-tested. Therefore, this paper aims to offer several hints for researchers that are looking for a starting point in the development of electrochemical sensors based on CPs and nanomaterials.

The resulting (bio)sensors were characterized by cyclic voltammetry (CV) and scanning electron microscopy (SEM). Furthermore, the figures of merit (sensitivity, limit of detection and dispersion of the results, among others) were the parameters used to assess the resulting electrochemical performance of the different modified biosensing devices.

In order to stablish a simple system for the sake of the discussion, dopamine (DA) was the analyte used as benchmark in this work. DA detection has been severely pursued due to its intimate relation with brain diseases, such as Parkinson or Alzheimer, among others. Although DA is an electroactive molecule that can be easily measured with regular sensors, the interferent species, such as ascorbic acid (AA), possess an oxidation potential very close to the one corresponding for DA; nonetheless the concentration of AA in brain tissue is much higher than DA, what makes the DA detection in human samples very challenging [34]. A plausible alternative is the use of a biosensor that provides the required selectivity. Thus, tyrosinase-based biosensors are really promising tools for this purpose. Lastly, the modified biosensors with better figures of merits were used in the determination of DA in synthetic and real samples (Zentiva, a drug for brain diseases), as well as for carrying out interference studies.

2. Materials and Methods

2.1. Reagents and Chemicals

Hydrochloric acid and dipotassium hydrogen phosphate were obtained from Panreac (Barcelona, Spain). Methyltrimetoxisilane (MTMOS), sulfuric acid and potassium dihydrogen phosphate were purchased from Merck (Darmstadt, Germany). Graphite powder UF was supplied by Alfa Aesar (Karlsruhe, Germany). 3,4-ethylenedioxythiophene, potassium tetrachloroaurate (III), tyrosinase (E.C. 1.14.18.1, from mushroom, 3610 units/mg solid), potassium hexacyanoferrate (II), potassium hexacyanoferrate (III), hydroquinone, epinephrine and multiwalled-carbon nanotubes were obtained from Sigma (Steinheim, Germany). Sodium citrate trihydrate was purchased from Scharlau (Scharlau Chemie, Sentmenant, Spain). Dopamine hydrochloride was supplied by Fluka (Buchs SG. Switzerland). All these reagents were used in the analytical grade without further pretreatment. Real sample of dopamine hydrochloride (5 mg/mL) concentrate solution for intravenous infusion was from Zentiva (Bucharest, Romania). All aqueous solutions were prepared with nanopure water, which was obtained by passing deionized water through a Milli-Q system (18 MΩ·cm, Millipore, Bedford, MA, USA).

2.2. Synthesis and Characterization of AuNPs

The synthesis of gold nanoparticles (AuNPs) was performed employing a QSONICA Q700 from MISONIX (600 W, 20 KHz, 13 mm titanium tip) (New York, NY, USA) by using the previously published procedure [35]. UV-Visible measurements were made using a PG Instrument, T80+ (Leicestershire, United Kingdom) and a Microtrac Nanotrac Wave particle analyser (780 nm, 3 mW) (Meerbusch, Germany) was used to obtain the particle size distribution of gold nanoparticles. Once the AuNPs were synthesized and characterized, they were stored in dark at room temperature.

2.3. Electrochemical Measurements

All electrochemical measurements were performed using an Autolab potentiostat /galvanostat 302 N (Ecochemie, Utrecht, The Netherlands) equipped with FRA2 module, in a three-electrode configuration. The working electrodes were made of Sonogel-Carbon electrodes (SNGC), with an inner diameter of 1.15 mm, prepared according to a previously published procedure [36]. The reference electrode was an Ag/AgCl/KCl (3 M) electrode (Metrohm, Herisau, Suiza). A platinum rod (Metrohm, Herisau, Suiza) was employed as the counter electrode. Before being used, the working SNGC electrodes were electrochemically

polarized in 0.1 M H_2SO_4 aqueous solution by two polarization steps at −0.7 V for 10 s, and at +1.8 V for 10 s, respectively [32]. This electrochemical procedure was repeated four times. The electrochemical characterization of the working electrodes was achieved using cyclic voltammetry (CV). To perform CV assays, potassium hexacyanoferrate (III) was used as the redox probe. The cyclic voltammograms were recorded in the potential range from −0.2 to +0.5 V, at the scan rate potential of 50 $mV \cdot s^{-1}$. The quantitation of the analytes was performed by CV in the potential range from −0.2 to +0.5 V, in an air-saturated buffered aqueous solution.

2.4. Modification of the SNGC Electrode Surface

The electrode materials generated can be understood as a result of two contributions, the species involved during the electrodeposition and the electrodeposition method itself. The diversity of conditions selected to examine the former contribution is collected in Table 1. Regarding the latter, SV and SC methodologies are employed as electrodeposition approaches. In order to be able to compare the results, only one set of parameters is employed for each methodology, which is explained as follows. Scheme 1 exposes the main idea of the preparation of the (bio)sensors as well as their working principle.

Table 1. Different modification conditions performed on the SNGC electrodes.

Configuration	Type of Modification	Procedure
C1	SNGC/AuNPs (drop)	4.1 µL of freshly synthesized AuNPs were drop-casted onto the surface of a pre-treated SNGC electrode. The electrode was allowed to dry overnight in a dark chamber at room temperature.
	Sinusoidal Voltage based sensors	
C2	SNGC/PEDOT-SV	The electrodeposition of PEDOT layer was performed from an aqueous solution containing the optimum concentrations of 0.01 M EDOT, and 0.05 M phosphate buffer solution (PBS) at pH 7.
C3	SNGC/PEDOT+Tyr-SV	The electrodeposition of PEDOT-Tyr layers was done from an aqueous solution containing the optimum concentrations of 0.01 M EDOT, 2 mg/mL of Tyr, and 0.05 M phosphate buffer solution (PBS) at pH 7 [33].
C4	SNGC/AuNPs (drop)/PEDOT+Tyr-SV	A SNGC/AuNPs (drop-casted) sensor was modified employing the procedure described in C3.
C5	SNGC/PEDOT+Tyr-SV/AuNPs (drop)	A SNGC/PEDOT-Tyr-SV biosensor was modified employing the procedure of SNGC/AuNPs(drop-casted) previously used in C1.
C6	SNGC/AuNPs (Electrogen)/PEDOT+Tyr-SV	A bare SNGC electrode was immersed in a solution of 5 mL containing 1.5 mM $KAuCl_4$, 0.1 M KCl and 0.1 M H_2SO_4. A chronoamperometry technique was used applying 0.18 V for 200 s. After that, the electrode was polarized in a solution of 0.05 M H_2SO_4 by cyclic voltammetry with a potential step from 0.0 to 1.5 V and scan rate of 50 mV/s for 5 cycles. Then, the electrodeposition of PEDOT-enzyme layer was performed using the same previous protocol abovementioned in C3 [37].
C7	SNGC/AuNPs (Electrochem)/PEDOT+Tyr-SV	A SNGC electrode was immersed in 2.4 mL of a solution containing 200 µL of AuNPs, 0.01 M EDOT, 2 mg/mL of Tyr, and 0.05 M phosphate buffer solution (PBS) at pH 7. After that, the Sinusoidal Voltage procedure was applied.
C8	SNGC/PEDOT-SV/AuNPs (drop)	A SNGC/PEDOT-SV sensor was modified employing the procedure of SNGC/AuNPs (drop-cast) previously mentioned in C1.

Table 1. *Cont.*

Configuration	Type of Modification	Procedure
C9	SNGC/PEDOT-SV/[CNTsAuNPs]	2 mL of a solution containing 1.5 mL of AuNPs, and 1 mg·mL^{-1} CNTs in 0.05 M PBS pH 7 was placed in a vial. The mixture was stirred by vortex for 20 min. After centrifugation (2 min, 10,000 rpm at 20 °C) the solid phase was added into a 0.01 M EDOT and 0.05 M PBS pH 7 solution. Finally, a SNGC electrode was immersed in the solution and electrodeposited following the procedure for SNGC/PEDOT-SV abovementioned in C2.
C10	SNGC/PEDOT-SV/CNTs-AuNPs	A SNGC electrode was immersed in a 5 mL solution containing 0.01 M EDOT, 1 mg·mL^{-1} CNTs and 200 µL of AuNPs in 0.05 M PBS pH 7; this solution was previously sonicated for 2 min. Later, the electrodeposition was performed using C2 procedure.
C11	SNGC/PEDOT-SV/CNTs	The modification procedure was similar to the one described for C10 but without AuNPs in the initial mixture.
C12	SNGC/PEDOT+Tyr-SV/CNTs	The procedure of this modification is similar to the one explained in C11 but with the addition of 2 mg·mL^{-1} of Tyr in the initial solution.
C13	SNGC/PEDOT+Tyr-SV/CNTs-AuNPs	The modification procedure in this case follows the same steps than the one performed in C12. Nevertheless, 200 µL of AuNPs were added to the mixture before the electrodeposition.
C14	SNGC/PEDOT-SV/[CNTsAuNPs] (drop)	Following the procedure to attach AuNPs in CNTs described in C9, the CNTs-AuNPs nanocomposite solution is obtained. 4.1 µL are drop-casted onto the surface of a SNGC/PEDOT-SV. The electrode was allowed to dry overnight in a dark chamber at room temperature.
Sinusoidal Current based sensors		
C15	SNGC/PEDOT+Tyr-SC	The electrodeposition of PEDOT-Tyr layers was performed from an aqueous solution containing the optimum concentrations of 0.01 M EDOT, 2 mg·mL^{-1} of Tyr, and 0.05 M phosphate buffer solution (PBS) at pH 7, using the SC procedure [33].
C16	SNGC/PEDOT-SC/CNTs	A SNGC electrode was immersed in a 5 mL solution containing 0.01 M EDOT, 1 mg·mL^{-1} CNTs in 0.05 M PBS pH 7; this solution was previously sonicated for 2 min. Later, the electrodeposition was carried out by using C15 procedure
C17	SNGC/PEDOT-SC/AuNPs (drop)	A SNGC/PEDOT-SC sensor was modified employing the procedure for C1.
C18	SNGC/AuNPs (drop)/PEDOT+Tyr-SC	In this case, C1 electrode was modified by using the procedure described in C15.
C19	SNGC/PEDOT+Tyr-SC/AuNPs (drop)	4.1 µL of freshly synthesized AuNPs were drop-casted onto the surface of the SNGC/PEDOT+Tyr-SC biosensor as explained in C1.

The terminology of the resulting sensor aims to aid their easy identification; according to this, the name is expressed in a simple manner where the layers are written from the inner to the outside of the electrode ordered, from left to right and separated by slashes. For example, SNGC/PEDOT+Tyr-SV/AuNPs (drop) can be understood as a SNGC electrode with a layer of PEDOT and tyrosinase deposited onto the surface by SV, where AuNPs have been lastly deposited by drop-casting methodology. SNGC: Sonogel-Carbon; AuNPs: gold nanoparticles; PEDOT: poly(3,4-ethylenedioxythiophene); SV: sinusoidal voltage; Tyr: tyrosinase; CNTs: carbon nanotubes; SC: sinusoidal current.

Concerning the sinusoidal voltage procedure, the electrodeposition of the CPs layer was performed using a SNGC electrode and the FRA software manual control features of the potentiostat by using a 50 mHz fixed frequency value, with excitation amplitude (ΔE_{ac}) of ±0.35 V, applying a fixed d.c. potential (E_{dc}) value of 0.60 V and a deposition time of 300 s [33].

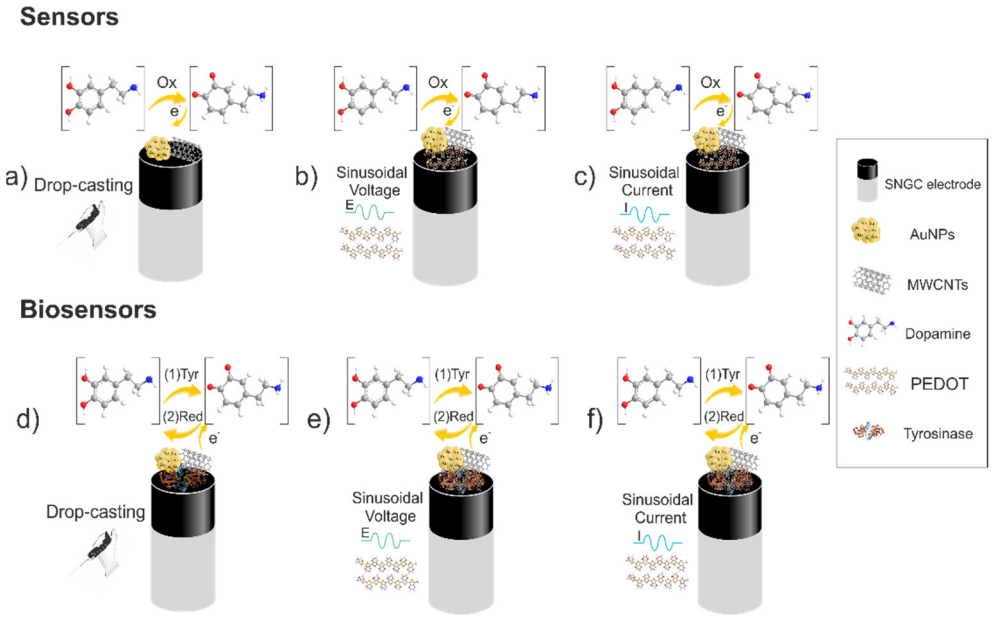

Scheme 1. Diagram of the preparation of the sensors and biosensors and their proposed working principle for the determination of dopamine: (**a**) drop-casting based sensor by using gold nanoparticles and multiwalled carbon nanotubes; (**b**) 3,4-ethylenedioxythiophene electrodeposited based sensor via sinusoidal voltage incorporating gold nanoparticles and multiwalled carbon nanotubes; (**c**) 3,4-ethylenedioxythiophene electrodeposited based sensor via sinusoidal current incorporating gold nanoparticles and multiwalled carbon nanotubes; (**d**) drop-casting tyrosinase based biosensor by using gold nanoparticles and multiwalled carbon nanotubes; (**e**) 3,4-ethylenedioxythiophene electrodeposited tyrosinase based biosensor via sinusoidal voltage incorporating gold nanoparticles and multiwalled carbon nanotubes; (**f**) 3,4-ethylenedioxythiophene electrodeposited tyrosinase based biosensor via sinusoidal current incorporating gold nanoparticles and multiwalled carbon nanotubes.

Regarding the sinusoidal current procedure, the electrodeposition was similarly carried out on a SNGC by using the FRA software manual control features of the potentiostat, but selecting 100 mHz fixed frequency value, with excitation amplitude (ΔE_{ac}) of ± 1 μA, applying a fixed d.c. current (E_{dc}) value of 4 μA and a deposition time of 300 s [32].

2.5. Analytical Measurements

The benchmark analyte, dopamine, was quantified by using cyclic voltammetry in air-saturated aqueous buffer solution (pH 7) at room temperature employing the following analytical procedure: the response of the (bio)sensor studied toward the addition of several aliquots of analyte was recorded. For the interference studies, ascorbic acid (AA), hydroquinone (HQ) and epinephrine (EPI) were employed as interferents in the determination of dopamine by using two different concentration levels: 500 μM and 1000 μM, respectively. The standard addition method was used in the analytical determination of dopamine from Zentiva pharmaceutical drug. For this purpose, a volume of 20 mL, 0.1 M PBS was spiked with a known volume of dopamine chloride concentrated solution from a Zentiva vial in order to reach 50 μM of dopamine concentration into the cell, and then the voltammetric response of the biosensor was recorded. Then, three aliquots (100 μL, 10 mM each) of dopamine standard solution were added and the voltammetric response was registered after the addition of each aliquot. All the measurements were carried out by triplicate.

2.6. Surface Characterization by SEM

Scanning electron microscopy (SEM) studies were carried out on a FEI Nova NANOSEM 450 equipment (resolution = 1 nm). The micrographs were taken at 5 kV, with the sample

previously deposited onto a grid using two different detectors: secondary electron detector (ESD) and backscattered electron detector (CBS).

3. Results and Discussion

3.1. Characterization of AuNPs Synthesized by Ultrasound-Assisted Synthesis

The red wine-colored colloidal solution obtained from the ultrasound synthesis was firstly characterized by UV-Vis spectroscopy. The UV-vis absorption spectrum for the AuNPs colloid, ranging from 400 to 900 nm, is exposed in Figure 1A. A band located at 527 nm can be appreciated, very close to the characteristic surface plasmon resonance band of gold nanoparticles, located around 530 nm. The existence of this band is indicative of the presence of AuNPs. In order to characterize the AuNPs in depth, dynamic light scattering (DLS) studies were carried out and results are shown in Figure 1B. Weighted mean was used to determine the average size of the distribution and its standard deviation, so 9 ± 5 nm (with an 85% of the population comprised between 5 and 10 nm) were the resulting values. They are in consonance with the previous ones published using this synthesis procedure [35]. The AuNPs have a narrow range of size, making them a good candidate for the modification of the (bio)sensors proposed.

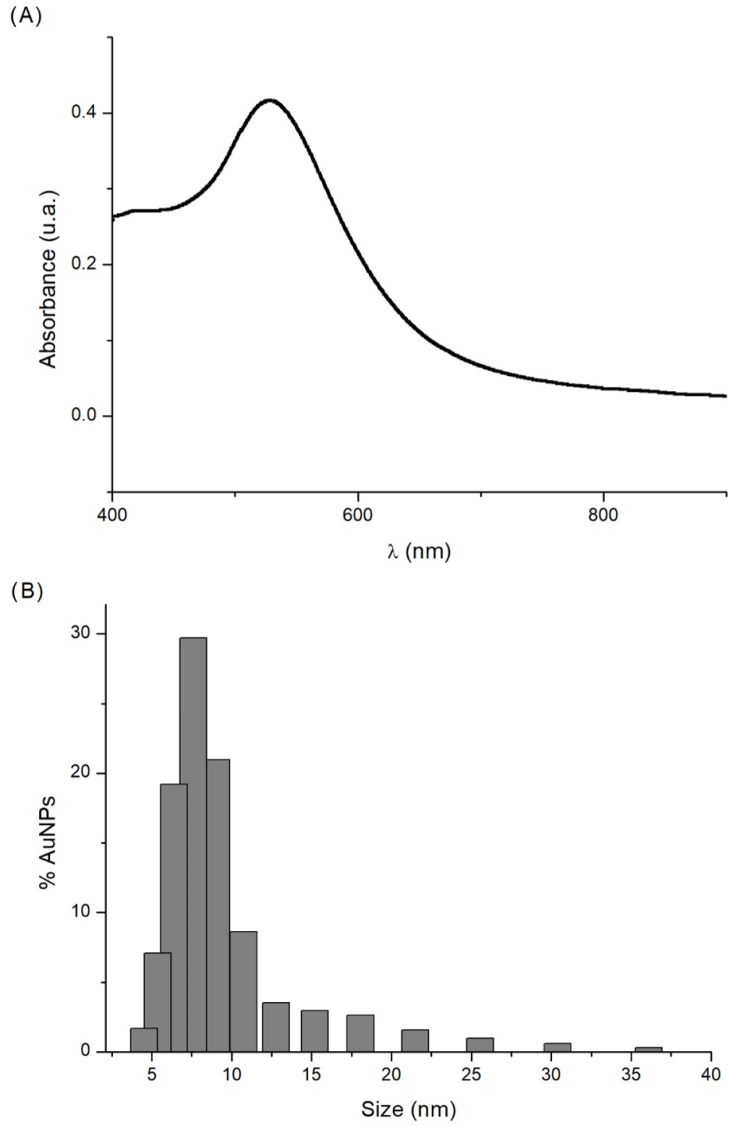

Figure 1. (**A**) UV-vis absorption spectrum for AuNPs aqueous solution and (**B**) size distribution histogram of AuNPs recorded by DLS technique.

3.2. Electrochemical Characterization of the Proposed (Bio)Sensors

Cyclic voltammetry (CV) was applied as the characterization technique for the bare electrodes and the (bio)sensors proposed. The measurements were performed in an aqueous solution containing both forms of the potassium hexacyanoferrate redox couple at equal concentrations. As an example, the cyclic voltammograms recorded using SNGC/PEDOT+Tyr-SC/AuNPs (drop) and SNGC bare electrodes are shown in Figure 2.

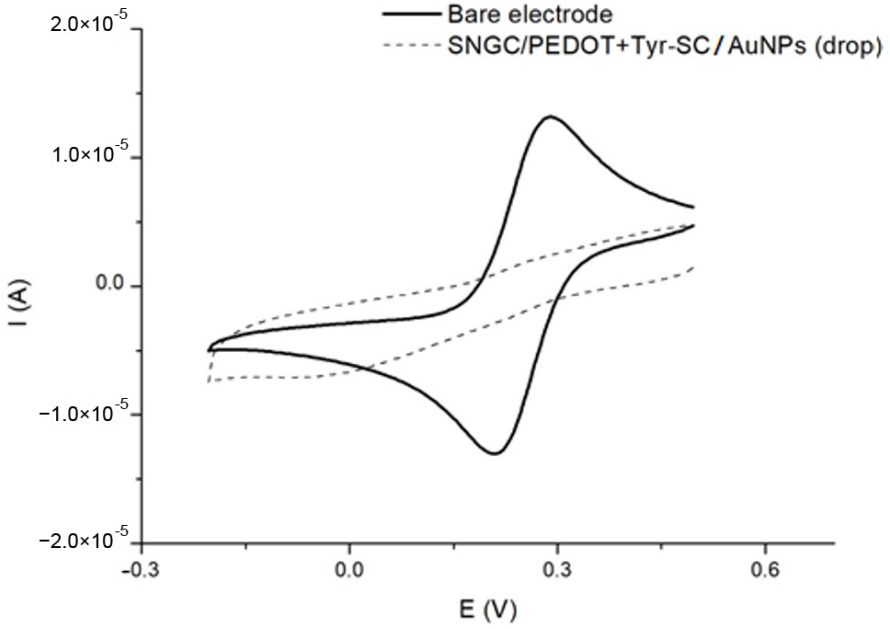

Figure 2. Electrochemical characterization of PEDOT-tyrosinase/Sonogel-Carbon (sinusoidal current-electrodeposited) biosensor modified with drop-casted AuNPs (SNGC/PEDOT+Tyr-SC/AuNPs (drop) (dashed line) and a bare SNGC electrode (bold) in an aqueous solution containing 5 mM $K_4Fe(CN)_6/K_3Fe(CN)_6$ and 1 M KCl by using CV.

Regarding the CVs exposed in Figure 2, the bare electrode voltammogram shows well-defined anodic and cathodic peaks around 0.2 and 0.3 V, respectively. These peaks are attributed to the redox pair, ferro/ferricyanide. On the other hand, the modified SNGC/PEDOT+Tyr-AuNPs presents the same peaks but shifted and attenuated. This could be explained by the decrease in the conductivity and the charge transfer due to the deposition of the enzyme onto the surface [33].

3.3. SEM Characterization

In Figure 3, SEM micrographs at different magnifications (80× and 600×) corresponding to the SNGC/PEDOT+Tyr-SC/AuNPs (drop) biosensor are shown. Besides, Figure 3A,C correspond to micrographs obtained with the secondary electron detector, while micrographs Figure 3B,D were recorded with the concentric backscattered electron (CBS) detector, using the same magnifications, respectively. In Figure 3A the polymeric matrix onto the surface of the electrode can be noticed. On the other hand, gold nanoparticles seem to be spread on the surface. This statement is corroborated by Figure 3B, where the BSE detector clearly shows groups of higher weight granulated bodies (white contrast). The higher weight can be only attributed to the Au atoms of AuNPs, unlike C, O, Si, and H atoms from the sonogel matrix that appear in dark-grey color. Regarding to the micrographs at 600× magnification (Figure 3C) the polymer matrix can be observed covering the biosensor; in this case AuNPs are not so evident. However, Figure 3D shows high weight bodies (white aggregates) over the entire polymeric matrix. Thus, AuNPs deposition on the biosensor surface may be also confirmed.

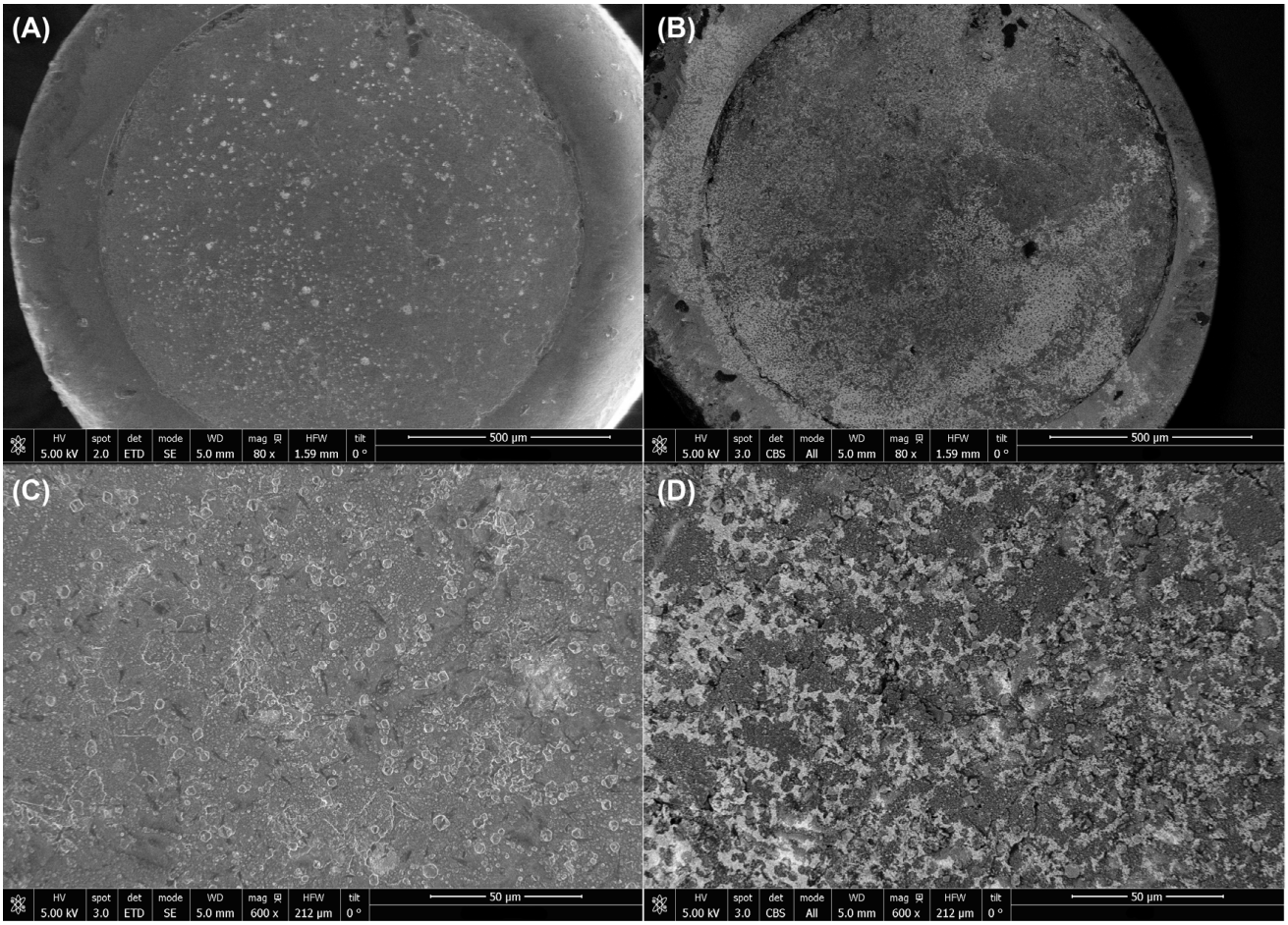

Figure 3. SEM micrographs of the SNGC/PEDOT+Tyr-SC/AuNPs (drop) biosensor: (**A**) AuNPs at lower magnification (80×) and secondary electron detector, (**B**) AuNPs at lower magnification (80×) and backscattered electron detector, (**C**) AuNPs at higher magnification (600×) and secondary electron detector and (**D**) AuNPs at higher magnification (600×) and backscattered electron detector.

3.4. Analytical Performance

3.4.1. Plain Examination of the Figures of Merit Observed

The analytical performance of the modified (bio)sensors developed in this work was investigated using dopamine as benchmark analyte. As an example, Figure 4 exposes the cyclic voltammograms recorded with a SNGC/PEDOT+Tyr-SC/AuNPs (drop) in a buffer aqueous solution in presence of different concentrations of dopamine, ranging from 20 µM to 300 µM. The cathodic peak, located around 0.18 V, was used to determine the concentration of dopamine due to the enzymatic conversion of this compound into its respective quinone. The figures of merit of all modified (bio)sensors were calculated. The linear range employed was from 20 µM to 300 µM in all cases. The sensitivity was determined using the slope of the corresponding calibration plot. Limit of detection (LOD) and limit of quantitation (LOQ) were calculated employing the criteria: 3·s/m for LOD and 10·s/m for LOQ, respectively, where s is the standard error of the regression line intercept and m is the slope of the calibration plot [38,39]. In order to determine the reproducibility of the biosensors, three different devices (n = 3) were used to calculate the relative standard deviation (RSD) of the slope and the LOD of the corresponding configuration. In Table 2, the figures of merit for all the configurations are summarized.

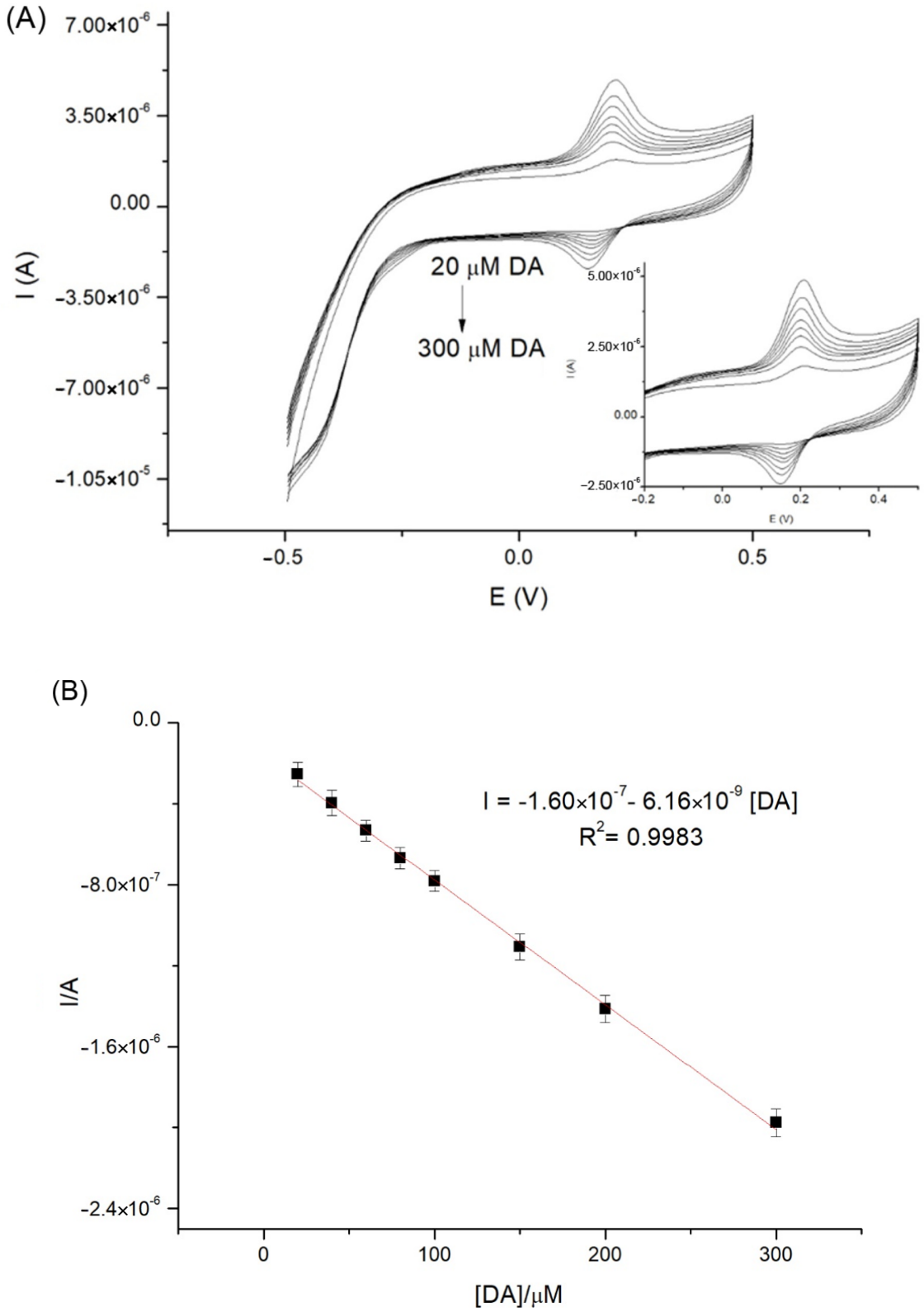

Figure 4. (**A**) Cyclic voltammograms recorded with a SNGC/PEDOT+Tyr-SC/AuNPs (drop) biosensor in 0.1 M PBS pH 7, with different dopamine concentrations ranging from 20 to 300 μM (20, 40, 60, 80, 100, 150, 200, 300), and (**B**) the corresponding calibration plot with the fitting equation and the determination coefficient (R^2). Error bars correspond to three replicates (n = 3).

Table 2. Figures of merit obtained with the different modified (bio)sensors generated.

Configuration	Type of Modification	R^2	Sensitivity ($A \cdot \mu M^{-1}$)	$RSD_{sensitivity}$ (%)	LOD (μM)	RSD_{LOD} (%)	LOQ (μM)
C1	SNGC/AuNPs (drop)	0.999	-2.65×10^{-9}	19.60	2.05	49.22	6.84
			Sinusoidal Voltage based sensors				
C2	SNGC/PEDOT-SV	0.996	-7.39×10^{-9}	14.57	10.52	7.15	35.07
C3	SNGC/PEDOT+Tyr-SV	0.999	-3.96×10^{-9}	14.09	4.28	31.34	14.28
C4	SNGC/AuNPs (drop)/PEDOT+Tyr-SV	0.998	-6.75×10^{-9}	21.88	6.01	11.61	20.03
C5	SNGC/PEDOT+Tyr-SV/AuNPs (drop)	0.999	-5.02×10^{-9}	26.12	3.59	34.78	11.97
C6	SNGC/AuNPs (Electrogen)/PEDOT+Tyr-SV	0.999	-3.58×10^{-9}	19.68	5.74	12.06	19.15
C7	SNGC/AuNPs (Electrochem)/PEDOT+Tyr-SV	0.999	-2.92×10^{-9}	18.52	5.12	27.70	17.05
C8	SNGC/PEDOT-SV/AuNPs (drop)	0.999	-7.04×10^{-9}	1.27	4.67	11.49	15.58
C9	SNGC/PEDOT-SV/[CNTs-AuNPs]	0.999	-5.96×10^{-9}	20.97	5.03	11.90	16.76
C10	SNGC/PEDOT-SV/CNTs-AuNPs	0.999	-4.89×10^{-9}	5.23	6.92	3.09	23.06
C11	SNGC/PEDOT-SV/CNTs	0.999	-8.20×10^{-9}	45.79	2.36	3.76	7.87
C12	SNGC/PEDOT+Tyr-SV/CNTs	0.998	-4.72×10^{-9}	10.70	7.97	18.90	26.56
C13	SNGC/PEDOT+Tyr-SV/CNTs-AuNPs	0.998	-4.76×10^{-9}	11.46	8.98	10.47	29.93
C14	SNGC/PEDOT-SV /[CNTsAuNPs] (drop)	0.997	-5.32×10^{-9}	3.66	10.93	9.61	36.4
			Sinusoidal Current based sensors				
C15	SNGC/PEDOT+Tyr-SC	0.998	-5.35×10^{-9}	6.18	6.50	5.96	21.66
C16	SNGC/PEDOT-SC/CNTs	0.999	-6.10×10^{-9}	4.83	6.09	8.32	20.30
C17	SNGC/PEDOT-SC/AuNPs (drop)	0.997	-7.02×10^{-9}	9.95	8.03	8.03	26.77
C18	SNGC/AuNPs (drop)/PEDOT+Tyr-SC	0.997	-7.31×10^{-9}	4.16	8.79	9.22	29.30
C19	SNGC/PEDOT+Tyr-SC /AuNPs (drop)	0.999	-4.92×10^{-9}	1.60	5.56	6.10	18.53

SNGC: Sonogel-Carbon; AuNPs: gold nanoparticles; PEDOT: poly(3,4-ethylenedioxythiophene); SV: sinusoidal voltage; Tyr: tyrosinase; CNTs: carbon nanotubes; SC: sinusoidal current.

According to the results shown in Table 2, several aspects should be discussed. In general, for all the different configurations, the linear fitting (R^2 value) is excellent. Firstly, the deposition of AuNPs onto a classic SNGC electrode provides a good limit of detection and quantitation, but it implies high dispersion of the results (RSD values of slope and LOD much higher than in most cases). In general, the implementation of PEDOT implies lower dispersion (RSD values) in the results. With respect to SV electrodeposition, the SNGC/PEDOT-SV (C2) configuration offers the greatest sensitivity towards the analyte. Nevertheless, it possesses higher dispersion of the results. The high sensitivity can be explained by the fact that the conducting polymer increases the conductivity of the system. Moreover, the tyrosinase was not included in this configuration, and thus its conductivity is not reduced by a non-conductive element as in other configurations. To determine DA using this sensor, an oxidation process is required. It is well known that the oxidation products of dopamine oxidation have a strong trend to polymerize and form an insulating film on the electrode promoting the process known as fouling. This fouling may affect in the reduction of the signal and the electron transfer hindering [40]. Additionally, it

was demonstrated that electrochemical oxidation of neurotransmitters is ruled by inner sphere reaction with a critical role of surface adsorption [41]. Therefore, the polymerization of dopamine onto the surface compromises the repeatability of the sensor as the polydopamine thickness grows, explaining the higher dispersion in the results [42]. Another reasonable explanation for the high dispersion of the results is a possible and undesired overoxidation effect that the electrochemical polymerization of PEDOT can cause [43]. The overoxidized PEDOT has lower conductivity and may affect the analytical performance of the device. When including tyrosinase in the configuration SNGC/PEDOT+Tyr-SV (C3), the sensitivity decreases, but LOD and LOQ are improved together with RSD values, as expected. In order to study the effect of AuNPs deposition, C4 (AuNPs drop-casted before biolayer SV electrodeposition) and C5 (AuNPs drop-casted onto the SV electrodeposited biolayer) were compared. C4 offers higher sensitivity but lower LOD; regarding RSD values, there is not a clear trend. As it is well known, the sensitivity is related with the signal obtained. Thus, the higher signal obtained in AuNPs drop-casted before biolayer SV electrodeposition (C4) could be attributed to a higher conductivity supplied by a better attachment of AuNPs directly on the transducer surface, which is typical for this kind of nanomaterials that improve electron transfer and sensitivity of electronic processes [44]. Taking into account SNGC/AuNPs (Electrogen)/PEDOT+Tyr-SV (C6) and SNGC/AuNPs (Electrochem)/PEDOT+Tyr-SV (C7), low sensitivity towards DA in comparison with others can be appreciated. On the other hand, their sensitivity was higher than the one calculated for SNGC/AuNPs (drop) (C1). This result could be ascribed to a more homogenous and uniform distribution of AuNPs onto the surface of the electrode, leading to higher conductivity. Other reasonable explanation would be that the electrogeneration process provides a higher concentration of AuNPs than the electrodeposition one (figures of merits of SNGC/PEDOT+Tyr-SV (C3) and SNGC/AuNPs (Electrochem)/PEDOT+Tyr-SV (C7) are very similar, what could support this explanation: low efficiency of AuNPs incorporation in the biolayer). This higher concentration would increase the conductivity of the system and, hence, its sensitivity. In addition, SNGC/AuNPs (Electrogen)/PEDOT+Tyr-SV (C6) present a lower dispersion of the results. Thus, it could be assumed that the electrogeneration process integrates AuNPs in a more reproducible way than the procedure of SNGC/AuNPs (Electrochem)/PEDOT+Tyr-SV (C7). Concerning their LOD, no significant differences can be pointed out. Concerning the SNGC/PEDOT-SV/AuNPs (drop) (C8) configuration, the drop-casting of AuNPs onto the previously electrodeposited PEDOT layer seems to offer much improvement in the LOD and dispersion of the results, but sensitivity is not much affected, compared with SNGC/PEDOT-SV (C2).

The addition of CNTs does not seem related with a strong improvement in the parameters studied. Nevertheless, the RSD values of these configurations are, generally, lower than those obtained for other sensors, especially for SNGC/PEDOT-SV/CNTs-AuNPs (C10) and SNGC/PEDOT-SV/CNTs (C11). On the contrary, the configuration SNGC/PEDOT-SV/[CNTsAuNPs] (C9), where the CNTsAuNPs nanocomposite is used, a higher dispersion of the slope can be observed. On the other hand, C9 shows one of the highest sensitivities of CNTs modified (bio)sensors. This fact could be explained by the possible synergistic effect of the CNTs and AuNPs in the nanocomposite in comparison with the single nanomaterials. Regarding the LOD, C11 seems to be the best option of the entire list. Even with no enzyme or AuNPs the sensor shows outstanding parameters. This could indicate a certain grade of incompatibility of CNTs with other modifiers (at least in a non-nanocomposite form), tyrosinase or AuNPs. However, PEDOT layer would be suitable to use with CNTs. Concerning SNGC/PEDOT+Tyr-SV/CNTs-AuNPs (C13), the addition of AuNPs to this system does not provide such a big difference in the parameters studied. Besides, SNGC/PEDOT+Tyr-SV/CNTs (C12) and C13 do not show any remarkable parameters. Finally, SNGC/PEDOT-SV/[CNTsAuNPs] (drop) (C14) presents greater sensitivity, probably due to the synergistic effect of the nanocomposite, but one of the highest limits of detection. Despite this fact, it possesses the second lower slope dispersion. Thus, according to the results obtained and the previous discussion, it seems that electrodeposition

process should be done after drop-casting AuNPs onto the transducer surface. Besides, the simultaneous electrodeposition of a high number of components (monomer, enzyme and CNTs, AuNPs or nanocomposite) seems to decrease the efficiency of the process and the electrochemical performance of the (bio)device obtained, mainly when including the enzyme. However, RSD values could be improved by drop-casting the nanocomposite after electrodeposition.

The second part of Table 2 shows the analytical parameters obtained with (bio)sensors modified by using SC method. In a previous paper, SC has been established as an alternative of the SV method. This approach provides lower limit of detection, higher sensitivities and porous structure, among other advantages [33]. Thus, the application of SC to the sensors previously obtained with SV would lead to superior devices from the point of view of the electrochemical performance. To study the effect of SC in the sensors, several configurations were selected due to the relatively good results obtained with SV: SNGC/AuNPs (drop)/PEDOT+Tyr-SV (C4), SNGC/PEDOT+Tyr-SV/AuNPs (drop) (C5), SNGC/PEDOT-SV/AuNPs (drop) (C8) and SNGC/PEDOT-CV/CNTs (C11). From these devices, the best LOD was found for the SNGC/PEDOT-SV/CNTs (C11) sensor. However, the lack of selectivity of this sensor, due to the absence of the enzyme, was the main drawback of this configuration. In relation to the other devices, SNGC/PEDOT-SV/AuNPs (drop) (C8) stood out as the best modification, obtaining great sensitivity and a good LOD, minimizing the dispersion of the results. Nevertheless, the absence of enzymes would lead to the same disadvantage exposed in the previous case. The SNGC/PEDOT+Tyr-SV/AuNPs (drop) (C5) modifications offered good parameters in comparison with SNGC/AuNPs (drop)/PEDOT+Tyr-SV (C4), excepting for the RSD_{LOD}. In addition, SNGC/PEDOT+Tyr-SV (C3) was also included in SC electrodeposition to have a reference with no nanomaterial modifications.

Regarding the results of SC approaches (configurations from C15 to C19 in Table 2), an evident decrease in the dispersion of the results can be observed. However, the sensitivity and LOD did not expose such a clearly trend with respect to SV configurations. The electrode no modified with nanomaterials SNGC/PEDOT+Tyr-SC (C15) presents higher sensitivity and slightly higher LOD in comparison with its SV analogous (C3). However, the greatest contrast can be observed in the nice reduction of the $RSD_{sensitivity}$ and RSD_{LOD} values. A possible explanation is that SC method is more reproducible to incorporate the enzyme and the conducting polymer than SV among other advantages, as expected from previous studies [33]. The sensor modified only with PEDOT and CNTs SNGC/PEDOT-SC/CNTs (C16) does not show any improvement at all. Sensitivity, LOD, and the dispersion were clearly inferior to the one modified with SV SNGC/PEDOT-SV/CNTs (C11). A feasible explanation would be the higher roughness of the layer obtained with SC, which could cause some steric hindrance during the attachment of the CNTs leading to a lower load of nanotubes in the layer. SNGC/PEDOT-SC/AuNPs (drop) (C17) does not expose improvements in comparison with SNGC/PEDOT-SV/AuNPs (drop) (C8) neither. Even their parameters are slightly worse, especially the parameters related with the LOD. Regarding the experiments involving SNGC/AuNPs (drop)/PEDOT+Tyr-SC (C18) and SNGC/PEDOT+Tyr-SC/AuNPs (drop) (C19), both devices demonstrate improvement with respect to their analog in SV (C4 and C5), except for the LOD of C19, which is slightly lower. The most notorious improvement is the decrease of the dispersion in the results. In addition, C19 presented the lowest RSD values. In general, it seems that the sensors were less favored in the new SC approach than the biodevices though. Besides, in this case, it seems that drop-casting AuNPs before SC electrodeposition is also favored from the point of view the sensitivity of the devices. This fact can be explained similarly as previously mentioned with SV results. However, with the configuration SC-electrodeposition + AuNPs, drop-casting enhances LOD and RSD values.

The electrochemical performance for dopamine determination of the most relevant (bio)sensing configurations obtained was also assessed. Table 3 shows a comparison with other electrochemical sensors found in literature.

Table 3. Figures of merit obtained with different electrochemical (bio)sensors.

Electrode Material	LOD (μM)	Reference
SNGC/PEDOT-SV/CNTs (C11)	2.4	This work
SNGC/PEDOT+Tyr-SC/AuNPs (drop)(C19)	5.6	This work
Au-disk/PEDOT-tyrosinase	4.2	[45]
Graphene oxide/Fe_3O_4	0.48	[46]
Tyrosinase/NiO/ITO	1.04	[47]

SNGC: Sonogel-Carbon; AuNPs: gold nanoparticles; PEDOT: poly(3,4-ethylenedioxythiophene); SV: sinusoidal voltage; Tyr: tyrosinase; CNTs: carbon nanotubes; SC: sinusoidal current; ITO: indium tin oxide.

As exposed in the previous table, Sonogel Carbon/tyrosinase-based (bio)sensors display similar limit of detection values in comparison with other modified electrochemical sensors for dopamine sensing. Therefore, their analytical performance towards the benchmark analyte is demonstrated.

3.4.2. Statistical Studies of the Data by ANOVA

In order to obtain statistical differences among the configurations proposed in this work, an ANOVA with a significance level of 95% was performed. This ANOVA was performed by means of the LOD of the (bio)sensors prepared and it will aid to identify the possible role of the procedure and nanomaterials used in this research.

Generally, an *F*-test and *p*-value of 0.05 are employed to examine these variances. Briefly, *p*-values lower than 0.05 implies significant statistical differences with a 95% level of confidence. Nevertheless, the use of *p*-value as unique criteria to perform this differentiation has been criticized before, mainly due to interpretation errors [48]. Besides, this value only brings binary information either are or not significant differences without offering data concerning the magnitude of these differences. For these reasons, the *F*-statistic can bring also useful information and supplement the *p*-value. *F*-value relates the mean square for every factor with the mean squared total error, i.e., it is a variance comparison to identify significant statistical differences. Lesser differences provide lower *F*-values, on the contrary high differences are conversed into high *F*-values. Thus, not only can the presence of significant statistical differences be estimated using this value, but the magnitude of these differences as well [49].

For the sake of the discussion, the results have been analyzed in two different groups, either sensors or biosensors prepared.

Concerning the ANOVA applied for sensors, a high *F*-statistic value (66.76) was found, which indicates significant statistical differences between the arithmetic mean of each population. This fact is also corroborated by the low *p*-value (less than 0.001). In addition, the high value of *F* suggests particularly strong differences. Thus, it is also possible to establish that there is a strong influence in the LOD obtained regarding the manner of how sensors are modified with the selected nanomaterials. Figure 5 exposes the confidence intervals for the mean (Fisher least significance difference).

It seems that the composite CNTs-AuNPs drop-casted onto the surface (C14) do not provide an enhancement in the LOD of the resulting device in comparison with the devices modified with only one nanomaterial or even only with the conducting polymer. On the contrary there is, indeed, an improvement when the nanocomposite is electrodeposited altogether (SNGC/PEDOT-SV/[CNTs-AuNPs]) (C9). However, the LOD obtained is similar to the one resulting from the modification with only AuNPs drop-casted, as can be observed from configurations SNGC/PEDOT-SV/AuNPs (drop) (C8) and SNGC/PEDOT-SC/AuNPs (drop) (C17). In addition, it can be seen that last configuration present no difference with the one that includes both nanomaterials separated (CNTs and AuNPs) during the electrodeposition step in sinusoidal voltage methodology C8 and SNGC/PEDOT-SV/CNTsAuNPs (C11). Furthermore, it can be appreciated that the LOD of these agglutinated materials in SV are equivalent to the one obtained only with CNTs by using the SC (C16). Remarkably, the lowest LODs are found for SNGC/AuNPs (drop) (C1) and SNGC/PEDOT-SV/CNTs (C11), although there are no statistical differences

among them. It should be noticed that, despite the multiple options employed, a very simple configuration as C1 achieves the best results in terms of LOD. Therefore, it may be considered as the optimal configuration, also taking into account the simplicity and the lower cost involved in the preparation of the sensors.

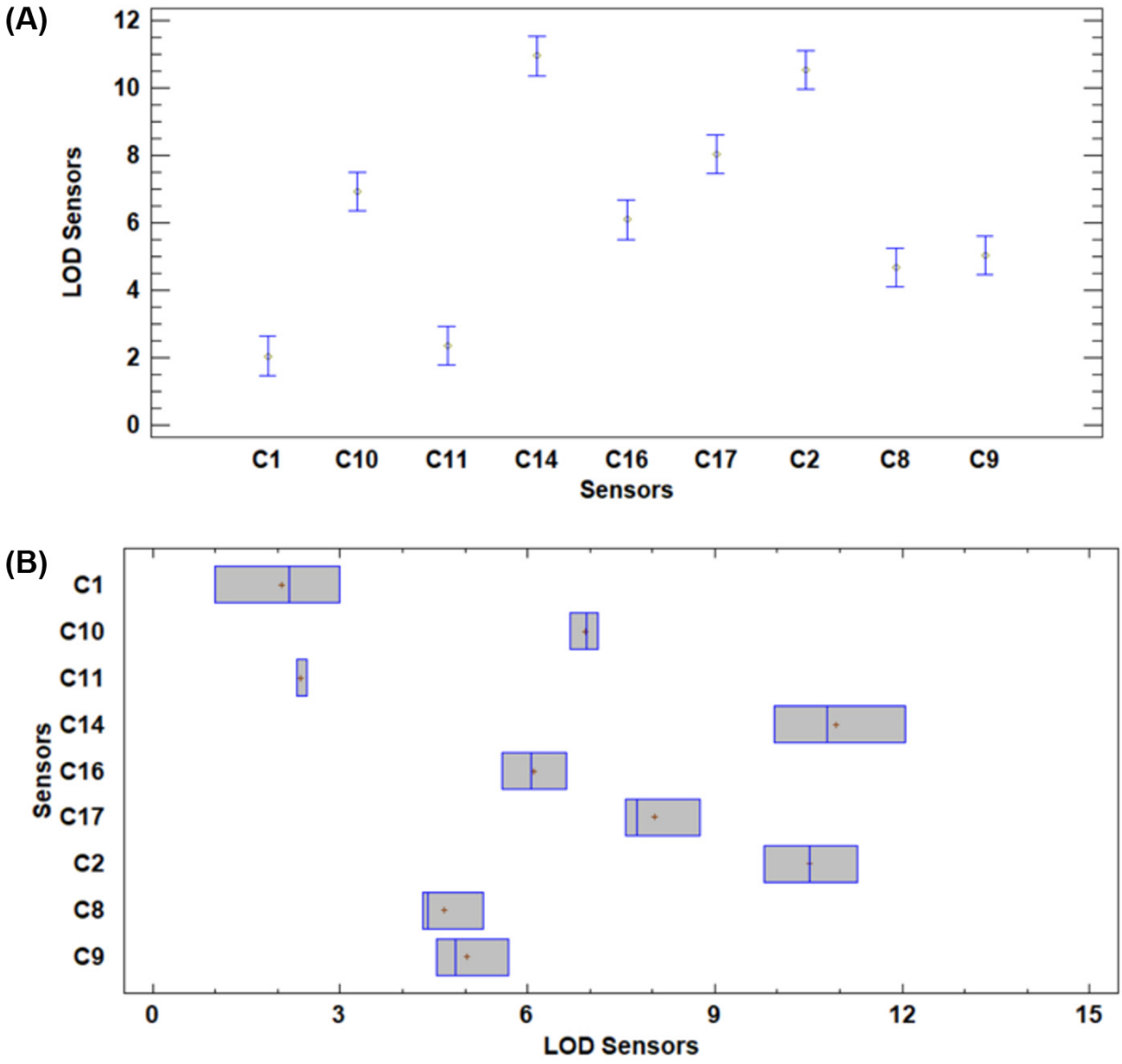

Figure 5. ANOVA graphs referred to the LOD (μM) and sensors prepared, confidence intervals for the mean (Fisher Least significance difference): (**A**) mean graphs and (**B**) box and whisker plot. SNGC/AuNPs (drop) (C1), SNGC/PEDOT-SV (C2), SNGC/PEDOT-SV/AuNPs (drop) (C8), SNGC/PEDOT-SV/[CNTsAuNPs] (C9), SNGC/PEDOT-SV/CNTs-AuNPs (C10), SNGC/PEDOT-SV (C11), SNGC/PEDOT-SV/[CNTsAuNPs] (drop) (C14), SNGC/PEDOT-SC/CNTs (C16), SNGC/PEDOT-SC/AuNPs (drop) (C17).

Regarding biosensors, an *F*-value (7.04) and a lower *p*-value than 0.05 (0.0001) were obtained, indicating the significant statistical differences between the mean of the population, so there are differences in the LOD obtained according to the nanomaterials and the procedure used to fabricate the biosensor. However, it should be also appreciated that the lower *F*-value in comparison with the sensor scenario (66.76) reveals that these differences are less pronounced. This can also be observed in Figure 6 where the confidence intervals for the mean (Fisher Least significance difference) are shown. Therefore, the nanomaterials

and how they are implemented have a greater influence in the case of sensors than in the case where an enzyme is placed on the device.

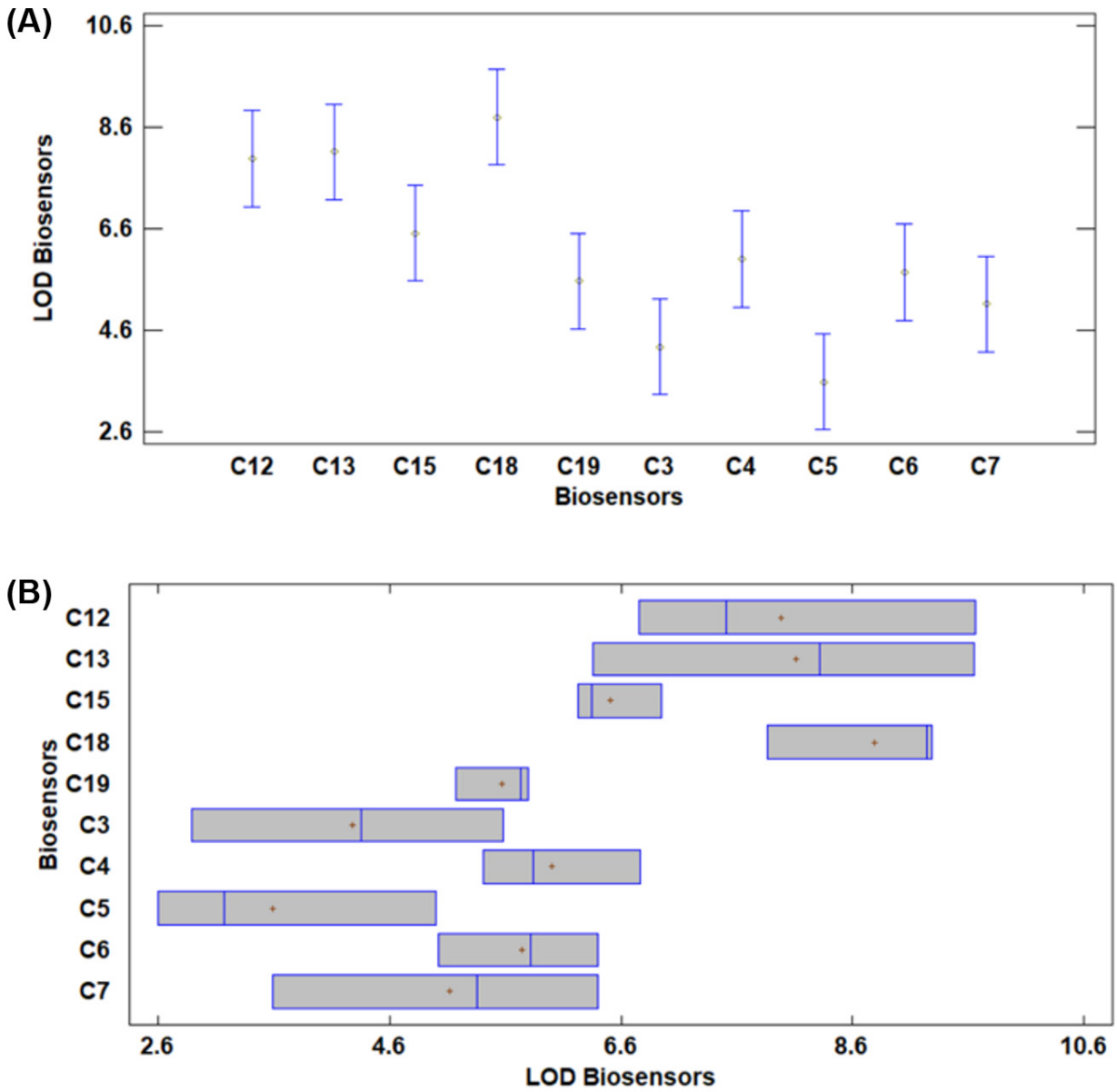

Figure 6. ANOVA graphs referred to the LOD (μM) and biosensors prepared, confidence intervals for the mean (Fisher Least significance difference): (**A**) mean graphs and (**B**) box and whisker plot. SNGC/PEDOT+Tyr-SV (C3), SNGC/AuNPs (drop)/PEDOT+Tyr-SV (C4), SNGC/PEDOT+Tyr-SV/AuNPs (drop) (C5), SNGC/AuNPs (Electrogen)/PEDOT+Tyr-SV (C6), SNGC/AuNPs (Electrochem)/PEDOT+Tyr-SV (C7), SNGC/PEDOT+Tyr-SV/CNTs (C12), SNGC/PEDOT+Tyr-SV/CNTs-AuNPs (C13), SNGC/PEDOT+Tyr-SC (C15), SNGC/AuNPs (drop)/PEDOT+Tyr-SC (C18), SNGC/PEDOT+Tyr-SC/AuNPs (drop) (C19).

In this case, as definitive a classification as in the previous case is not possible. Nonetheless, several aspects can be highlighted. SNGC/PEDOT+Tyr-SV/AuNPs (drop) (C5), SNGC/PEDOT+Tyr-SV (C3) and SNGC/AuNPs (Electrochem)/PEDOT+Tyr-SV seems to provide the lowest limit of detection although there are not differences between them. Very similar results are obtained for SNGC/PEDOT+Tyr-SC/AuNPs (drop) (C19), SNGC/AuNPs (Electrogen)/PEDOT+Tyr-SV (C6) and SNGC/AuNPs (drop)/PEDOT+Tyr-SV (C4). From these results it is possible to appreciate that there is not difference in the LOD

obtained either electrogenerating in situ the AuNPs or using some already prepared during the electrodeposition step. Besides, for the same electrodeposition process (sinusoidal voltage), the drop-casting of AuNPs has no impact in the resulting LOD; either the particles are drop-casted in the bare substrate or at the top of the electrode.

On the contrary, some differences can be recognized among the previous configurations and SNGC/PEDOT+Tyr-SV/CNTs (C12), SNGC/PEDOT+Tyr-SV/CNTs-AuNPs (C13) and SNGC/AuNPs (drop)/PEDOT+Tyr-SC (C18). It seems that the inclusion of CNTs leads to higher LOD in general terms. In addition, it should be also remarked that there are, indeed, differences between the resulting LOD according to the electrodeposition process, if the AuNPs are drop-casted onto the surface of the substrate.

Interestingly, the dispersion of the results in the biosensors is lower than in the case of the sensors prepared. It seems that the employment of the enzyme provides better repeatability, probably due to the significant role of the enzyme, which is integrated in reproducible ways, in the resulting devices.

3.5. Interference Studies

One of the aims of this paperwork was to propose a modified sensor to determine DA in real samples. For this purpose, C19 was selected as the best candidate to carry out this role. As it has been mentioned previously, C19 showed the lowest dispersion of the results, which can be translated into good repeatability of the measurements. It also offers a suitable LOD (5.56 μM); it is important to clarify that the real sample used in this paper contains 50 μM of DA. Furthermore, the endogenous concentration (human body) of DA measured is about 7.65 μM [34]. Thus, the biosensor proposed could be able to determine it as well. On the other hand, as exposed in Section 1, DA determination is challenging due to the presence of numerous interferents. This would be solved out employing an enzyme-based device. The enzyme allows the biosensor to discriminate the compounds present in the sample, providing the necessary selectivity to the system. Based on this purpose, a tyrosinase modified biosensor (C19) seems to be a good choice. Besides, interferent studies were performed employing typical substances (AA, HQ and EPI [34]). C15 (the non-nanomaterial modified biosensor) was used in the same assays for comparison purposes.

In Figures S2–S4 from the Supplementary Materials, the cyclic voltammograms registering the determination of dopamine in presence of the corresponding amount of the interferent (AA, HQ and EPI, respectively) are presented. Concerning the AA assays, the analytical signal corresponding to the electrochemical oxidation of ascorbic acid was found, while only the cathodic peak attributed to the reduction process of dopamine can be appreciated. Therefore, the determination of dopamine in presence of ascorbic acid is possible. In the case of HQ, a second cathodic peak can be observed around 2 mV due to the reduction of the oxidized resulting quinone. The distance between peaks is more than 100 mV, allowing a suitable determination of dopamine in presence of this interferent. Besides, for EPI assays, a second cathodic peak can be found around −216 mV due to the reduction of the oxidized product of epinephrine. As in the case of HQ, the cathodic peak is sufficiently separated to successfully determine dopamine in the presence of EPI. Finally, it is important to notice that there was no strong influence in the analytical signal of dopamine in the presence of foreign species at both concentration values tested. Consequently, both biosensors can be proposed as useful tools to determine dopamine in real samples.

3.6. Real Samples Analysis

A pharmaceutical product (Zentiva¸ solution for intravenous infusion, labeled concentrations 5 mg mL^{-1}) containing dopamine was analyzed using the standard addition method, as indicated in Section 2.5. These assays were carried out with both biosensors selected in Section 3.5 (C15 and C19), considered as the most relevant configurations tested from the point of view of the quality analytical parameters obtained in the previous screening. Regarding the results obtained for the SNGC/PEDOT+Tyr-SC (C15), a concentration of

55.30 ± 6.50 μM of DA was found. This implies a recovery percentage of 110.6%. This result supposes a very good value taking into account the existence of multiple and different species in the real sample, such as sodium metabisulphite, maleic acid, ethanol, propylene glycol, and sodium chloride, among others. In the case of SNGC/PEDOT+Tyr-SC/AuNPs) (drop) (C19), a concentration of 50.50 ± 4.63 μM of DA was found, involving a recovery of 101.0%. This result means that the biosensor modified with AuNPs offers much improvement and better results for real sample analysis.

4. Conclusions

In this study, a wide screening of multiple modifications of (bio)sensors based on electrodeposited PEDOT and nanomaterials by sinusoidal voltage and sinusoidal current approaches was performed. Each device obtained was employed to determine dopamine in a simple matrix in order to evaluate them in terms of sensitivity, LOD and RSD. The modification procedure as well as the modifiers employed were found to be relevant to the electrochemical performance of the resulting electrochemical devices. ANOVA studies were performed to assess the role of the nanomaterials employed and how they are integrated in the (bio)sensors. Several modifications stand out, such as the modification with AuNPs and CNTs without the presence of any enzyme. However, the most suitable results are found for the biosensor modified with AuNPs and generated by a sinusoidal current approach. Not only does it possess excellent analytical parameters, but it provides an important selectivity to the system as well thanks to the biological part. On the other hand, interference studies proved that this SC-based device may be used to determine dopamine in real and more complex matrices. This hypothesis was corroborated by the application of the biosensor in the determination of dopamine in a pharmaceutical preparation (Zentiva), with satisfactory recovery values. Above all, one idea should be remarked. Despite the first impression that a sensor prepared with both CNTs and AuNPs either separated or as nanocomposite would provide higher analytical performance, we have found that this is untrue for our case. The synergistic effect of the AuNPs-PEDOT-Tyrosinase group overcame all other configurations in general terms. Therefore, the selection of the modification approach may not be so straightforward, and it should be carefully revised according to the final aim because even small details have an impact on the generated device.

Supplementary Materials: The following supporting information can be downloaded at: https://www.mdpi.com/article/10.3390/chemosensors10080316/s1, Figure S1: Picture of a tyrosinase and gold nanoparticles-modified SNGC electrode by using drop-casting method; Figure S2: Cyclic voltammograms for the determination of dopamine in presence of different concentrations of AA, using a SNGC/PEDOT+Tyr-SC biosensor: (A) 500 μM and (B) 1000 μM, and a SNGC/PEDOT+Tyr-SC/AuNPs) (drop) biosensor: (C) 500 μM and (D) 1000 μM; Figure S3: Cyclic voltammograms for the determination of dopamine in presence of different concentrations of HQ, using a SNGC/PEDOT+Tyr-SC biosensor: (A) 500 μM and (B) 1000 μM, and a SNGC/PEDOT+Tyr-SC/AuNPs (drop) biosensor: (C) 500 μM and (D) 1000 μM; Figure S4: (A) Cyclic voltammograms for the determination of dopamine in presence of different concentrations of EPI, using a SNGC/PEDOT+Tyr-SC biosensor: (A) 500 μM and (B) 1000 μM), and a SNGC/PEDOT+Tyr-SC/AuNPs (drop) biosensor: (C) 500 μM and (D) 1000 μM.

Author Contributions: Conceptualization, M.T.R., J.M.P.-S., J.J.G.-G. and L.M.C.-A.; methodology, M.T.R., J.J.G.-G. and D.L.-I.; validation, M.T.R., A.S.-P. and D.L.-I.; formal analysis, M.T.R., A.S.-P., J.J.G.-G. and J.M.P.-S.; investigation, M.T.R., A.S.-P. and D.L.-I.; resources, D.B.-M., J.M.P.-S. and L.M.C.-A.; data curation, M.T.R., J.J.G.-G. and D.B.-M.; writing—original draft preparation, L.M.C.-A., J.J.G.-G., D.L.-I. and J.M.P.-S.; writing—review and editing, All; visualization, All; supervision, J.J.G.-G., J.M.P.-S. and L.M.C.-A.; project administration, J.M.P.-S. and L.M.C.-A.; funding acquisition, D.B.-M., J.M.P.-S. and L.M.C.-A. All authors have read and agreed to the published version of the manuscript.

Funding: Md. Towhidur Rahman thanks the European Commission (EACEA) for supporting his study and research activity inside the Erasmus Mundus Master in Quality in Analytical Laboratories (EMQAL) through an Erasmus Mundus studentship (SGA 2015-1992, FPA 2013-0225). J.J.

García-Guzmán thanks Instituto de Investigación Biomédica de Cádiz (INiBICA) for his post-doctoral contract framed in the Project ITI-0002-2019. D. López-Iglesias and A. Sierra-Padilla greatly acknowledge ESF funds, Sistema de Garantía Juvenil depending on Ministerio de Empleo y Seguridad Social of Spain and Junta de Andalucía for their employment contracts (E-11-20180043137). All the authors also acknowledge Junta de Andalucía (PAIDI 2020) and Institute of Research on Electron Microscopy and Materials (IMEYMAT—APPLIEDSENS, BIOSENSEP, POLYBIOSENS and NANO4(BIO)SENS projects) for their financial support. This research was co-financed by the 'Programa de Fomento e Impulso de la Investigación y de la Transferencia de la Universidad de Cádiz 2020-2021′ for the funds given through the project PR2020-013 (Proyectos de Investigación-Puente 2020).

Institutional Review Board Statement: Not applicable.

Informed Consent Statement: Not applicable.

Data Availability Statement: Not applicable.

Acknowledgments: Authors thank Electron Microscopy Division from Servicios Centrales de Investigación Científica y Tecnológica of University of Cadiz (SC-ICYT UCA) for their technical assistance during SEM measurements.

Conflicts of Interest: The authors declare no conflict of interest.

References

1. Shen, X.; Xia, X.; Du, Y.; Wang, C. Electroless Deposition of Au Nanoparticles on Reduced Graphene Oxide/Polyimide Film for Electrochemical Detection of Hydroquinone and Catechol. *Front. Mater. Sci.* **2017**, *11*, 262–270. [CrossRef]
2. Manan, F.A.A.; Hong, W.W.; Abdullah, J.; Yusof, N.A.; Ahmad, I. Nanocrystalline Cellulose Decorated Quantum Dots Based Tyrosinase Biosensor for Phenol Determination. *Mater. Sci. Eng. C* **2019**, *99*, 37–46. [CrossRef] [PubMed]
3. Kausaite-Minkstimiene, A.; Glumbokaite, L.; Ramanaviciene, A.; Dauksaite, E.; Ramanavicius, A. An Amperometric Glucose Biosensor Based on Poly (Pyrrole-2-Carboxylic Acid)/Glucose Oxidase Biocomposite. *Electroanalysis* **2018**, *30*, 1634–1644. [CrossRef]
4. Xu, H.; Zhou, S.; Jiang, D.; Chen, H.Y. Cholesterol Oxidase/Triton X-100 Parked Microelectrodes for the Detection of Cholesterol in Plasma Membrane at Single Cells. *Anal. Chem.* **2018**, *90*, 1054–1058. [CrossRef]
5. Cunha-Silva, H.; Arcos-Martinez, M.J. Dual Range Lactate Oxidase-Based Screen Printed Amperometric Biosensor for Analysis of Lactate in Diversified Samples. *Talanta* **2018**, *188*, 779–787. [CrossRef] [PubMed]
6. Phetsang, S.; Jakmunee, J.; Mungkornasawakul, P.; Laocharoensuk, R.; Ounnunkad, K. Sensitive Amperometric Biosensors for Detection of Glucose and Cholesterol Using a Platinum/Reduced Graphene Oxide/Poly(3-Aminobenzoic Acid) Film-Modified Screen-Printed Carbon Electrode. *Bioelectrochemistry* **2019**, *127*, 125–135. [CrossRef]
7. Nagles, E.; García-Beltrán, O.; Calderón, J.A. Evaluation of the Usefulness of a Novel Electrochemical Sensor in Detecting Uric Acid and Dopamine in the Presence of Ascorbic Acid Using a Screen-Printed Carbon Electrode Modified with Single Walled Carbon Nanotubes and Ionic Liquids. *Electrochim. Acta* **2017**, *258*, 512–523. [CrossRef]
8. Cui, L.; Lu, M.; Li, Y.; Tang, B.; Zhang, C. A reusable ratiometric electrochemical biosensor on the basis of the binding of methylene blue to DNA with alternating AT base sequence for sensitive detection of adenosine. *Biosens. Electron. B* **2018**, *102*, 87–93. [CrossRef]
9. Cui, L.; Shen, J.; Li, C.; Cui, P.; Luo, X.; Wang, X.; Zhang, C. Construction of a Dye-Sensitized and Gold plasmon-Enhanced Cathodic Photoelectrochemical Biosensor for Methyltransferase Activity Assay. *Anal. Chem.* **2021**, *93*, 10310–10316. [CrossRef]
10. Attar, A.; Cubillana-Aguilera, L.; Naranjo-Rodríguez, I.; de Cisneros, J.L.H.-H.H.; Palacios-Santander, J.M.; Amine, A. Amperometric Inhibition Biosensors Based on Horseradish Peroxidase and Gold Sononanoparticles Immobilized onto Different Electrodes for Cyanide Measurements. *Bioelectrochemistry* **2014**, *101*, 84–91. [CrossRef]
11. Attar, A.; Amine, A.; Achi, F.; Bacha, S.B.; Cubillana-Aguilera, L.; Palacios-Santander, J.M.; Baraket, A.; Errachid, A. A Novel Amperometric Inhibition Biosensor Based on HRP and Gold Sononanoparticles Immobilised onto Sonogel-Carbon Electrode for the Determination of Sulphides and Gold Sononanoparticles Immobilised Onto. *Int. J. Environ. Anal. Chem.* **2016**, *7319*, 1–15. [CrossRef]
12. Das, P.; Das, M.; Chinnadayyala, S.R.; Singha, I.M.; Goswami, P. Recent Advances on Developing 3rd Generation Enzyme Electrode for Biosensor Applications. *Biosens. Bioelectron.* **2016**, *79*, 386–397. [CrossRef] [PubMed]
13. Da Silva, W.; Ghica, M.E.; Ajayi, R.F.; Iwuoha, E.I.; Brett, C.M.A. Tyrosinase Based Amperometric Biosensor for Determination of Tyramine in Fermented Food and Beverages with Gold Nanoparticle Doped Poly(8-Anilino-1-Naphthalene Sulphonic Acid) Modified Electrode. *Food Chem.* **2019**, *282*, 18–26. [CrossRef]
14. Lupu, S.; Lete, C.; Javier del Campo, F. Dopamine Electroanalysis Using Electrochemical Biosensors Prepared by a Sinusoidal Voltages Method. *Electroanalysis* **2015**, *27*, 1649–1659. [CrossRef]
15. Buk, V.; Pemble, M.E. A Highly Sensitive Glucose Biosensor Based on a Micro Disk Array Electrode Design Modified with Carbon Quantum Dots and Gold Nanoparticles. *Electrochim. Acta* **2019**, *298*, 97–105. [CrossRef]

16. Çakıroğlu, B.; Demirci, Y.C.; Gökgöz, E.; Özacar, M. A Photoelectrochemical Glucose and Lactose Biosensor Consisting of Gold Nanoparticles, MnO_2 and g-C_3N_4 Decorated TiO_2. *Sens. Actuators B Chem.* **2019**, *282*, 282–289. [CrossRef]
17. Xuan, X.; Yoon, H.S.; Park, J.Y. A Wearable Electrochemical Glucose Sensor Based on Simple and Low-Cost Fabrication Supported Micro-Patterned Reduced Graphene Oxide Nanocomposite Electrode on Flexible Substrate. *Biosens. Bioelectron.* **2018**, *109*, 75–82. [CrossRef]
18. Stasyuk, N.; Gayda, G.; Zakalskiy, A.; Zakalska, O.; Serkiz, R.; Gonchar, M. Amperometric Biosensors Based on Oxidases and PtRu Nanoparticles as Artificial Peroxidase. *Food Chem.* **2019**, *285*, 213–220. [CrossRef]
19. Chauhan, N.; Tiwari, S.; Narayan, T.; Jain, U. Bienzymatic Assembly Formed @ Pt Nano Sensing Framework Detecting Acetylcholine in Aqueous Phase. *Appl. Surf. Sci.* **2019**, *474*, 154–160. [CrossRef]
20. Uribe, P.A.; Ortiz, C.C.; Centeno, D.A.; Castillo, J.J.; Blanco, S.I.; Gutierrez, J.A. Self-Assembled Pt Screen Printed Electrodes with a Novel Peroxidase Panicum Maximum and Zinc Oxide Nanoparticles for H_2O_2 Detection. *Colloids Surf. A Physicochem. Eng. Asp.* **2019**, *561*, 18–24. [CrossRef]
21. Malekzad, H.; Sahandi Zangabad, P.; Mirshekari, H.; Karimi, M.; Hamblin, M.R. Noble Metal Nanoparticles in Biosensors: Recent Studies and Applications. *Nanotechnol. Rev.* **2017**, *6*, 301–329. [CrossRef] [PubMed]
22. Lanzellotto, C.; Favero, G.; Antonelli, M.L.; Tortolini, C.; Cannistraro, S.; Coppari, E.; Mazzei, F. Nanostructured Enzymatic Biosensor Based on Fullerene and Gold Nanoparticles: Preparation, Characterization and Analytical Applications. *Biosens. Bioelectron.* **2014**, *55*, 430–437. [CrossRef] [PubMed]
23. Liu, C.; Chou, Y.; Tsai, J.; Huang, T. Applied Sciences Tyrosinase/Chitosan/Reduced Graphene Oxide Modified Screen-Printed Carbon Electrode for Sensitive and Interference-Free Detection of Dopamine. *Appl. Sci.* **2019**, *9*, 662. [CrossRef]
24. Barkauskas, J.; Mikoliunaite, L.; Paklonskaite, I.; Genys, P.; Petroniene, J.J.; Morkvenaite-Vilkonciene, I.; Ramanaviciene, A.; Samukaite-Bubniene, U.; Ramanavicius, A. Single-Walled Carbon Nanotube Based Coating Modified with Reduced Graphene Oxide for the Design of Amperometric Biosensors. *Mater. Sci. Eng. C* **2019**, *98*, 515–523. [CrossRef] [PubMed]
25. Canbay, E.; Akyilmaz, E. Design of a Multiwalled Carbon Nanotube-Nafion-Cysteamine Modified Tyrosinase Biosensor and Its Adaptation of Dopamine Determination. *Anal. Biochem.* **2014**, *444*, 8–15. [CrossRef]
26. Salazar, P.; Martín, M.; González-Mora, J.L. In Situ Electrodeposition of Cholesterol Oxidase-Modified Polydopamine Thin Film on Nanostructured Screen Printed Electrodes for Free Cholesterol Determination. *J. Electroanal. Chem.* **2019**, *837*, 191–199. [CrossRef]
27. Lete, C.; López-Iglesias, D.; García-Guzmán, J.J.; Leau, S.; Stanciu, A.; Marin, M.; Palacios-Santander, J.M.; Lupu, S.; Cubillana-Aguilera, L. A Sensitive Electrochemical Sensor Based on Sonogel-Carbon Material Enriched with Gold Nanoparticles for Melatonin Determination. *Sensors* **2021**, *22*, 120. [CrossRef]
28. Ghanam, A.; Haddour, N.; Mohammadi, H.; Amine, A.; Sabac, A.; Buret, F. A membrane-less Glucose/O_2 non-enzymatic fuel cell based on bimetallic Pd-Au nanostructure anode and air-breathing cathode: Towards micro-power applications at neutral pH. *Bionsens. Bioelectron.* **2022**, *210*, 114335. [CrossRef]
29. ElFadil, D.; Palmieri, S.; Silveri, F.; Della Pelle, F.; Sergi, M.; Del Carlo, M.; Amine, A.; Compagnone, D. Fast sonochemical molecularly imprinted polymer synthesis for selective electrochemical determination of maleic hydrazide. *Microchem. J.* **2022**, *180*, 107634. [CrossRef]
30. Ghanam, A.; Haddour, N.; Mohammadi, H.; Amine, A.; Sabac, A.; Buret, F. Nanoporous Cauliflower-like Pd-Loaded Functionalized Carbon Nanotubes as an Enzyme-Free Electrocatalyst for Glucose Sensing at Neutral pH: Mechanism Study. *Sensors* **2022**, *22*, 2706. [CrossRef]
31. García-Guzmán, J.J.; López-Iglesias, D.; Cubillana-Aguilera, L.; Bellido-Milla, D.; Palacios-Santander, J.M.; Marin, M.; Grigorescu, S.D.; Lete, C.; Lupu, S. Silver Nanostructures-Poly(3,4-Ethylenedioxythiophene) Sensing Material Prepared by Sinusoidal Voltage Procedure for Detection of Antioxidants. *Electrochim. Acta* **2021**, *393*. [CrossRef]
32. García-Guzmán, J.J.; López-Iglesias, D.; Cubillana-Aguilera, L.; Lete, C.; Lupu, S.; Palacios-Santander, J.M.; Bellido-Milla, D. Assessment of the Polyphenol Indices and Antioxidant Capacity for Beers and Wines Using a Tyrosinase-Based Biosensor Prepared by Sinusoidal Current Method. *Sensors* **2019**, *19*, 66. [CrossRef] [PubMed]
33. García Guzmán, J.J.; Aguilera, L.C.; Milla, D.B.; Rodríguez, I.N.; Lete, C.; Palacios Santander, J.M.; Lupu, S. Development of Sonogel-Carbon Based Biosensors Using Sinusoidal Voltages and Currents Methods. *Sens. Actuators B Chem.* **2018**, *255*, 1525–1535. [CrossRef]
34. Ribeiro, J.A.; Fernandes, P.M.V.; Pereira, C.M.; Silva, F. Electrochemical Sensors and Biosensors for Determination of Catecholamine Neurotransmitters: A Review. *Talanta* **2016**, *160*, 653–679. [CrossRef] [PubMed]
35. Cubillana-Aguilera, L.M.; Franco-Romano, M.; Gil, M.L.A.; Naranjo-Rodríguez, I.; Hidalgo-Hidalgo De Cisneros, J.L.; Palacios-Santander, J.M. New, Fast and Green Procedure for the Synthesis of Gold Nanoparticles Based on Sonocatalysis. *Ultrason. Sonochem.* **2011**, *18*, 789–794. [CrossRef] [PubMed]
36. Bellido-Milla, D.; Cubillana-Aguilera, L.M.; El Kaoutit, M.; Hernández-Artiga, M.P.; Hidalgo-Hidalgo De Cisneros, J.L.; Naranjo-Rodríguez, I.; Palacios-Santander, J.M. Recent Advances in Graphite Powder-Based Electrodes. *Anal. Bioanal. Chem.* **2013**, *405*, 3525–3539. [CrossRef] [PubMed]
37. Hilali, N.; Ghanam, A.; Mohammadi, H.; Amine, A.; García-Guzmán, J.J.; Cubillana-Aguilera, L.; Palacios-Santander, J.M. Comparison between Modified and Unmodified Carbon Paste Electrodes for Hexavalent Chromium Determination. *Electroanalysis* **2018**, *30*, 2750–2759. [CrossRef]

38. Shrivastava, A. Methods for the determination of limit of detection and limit of quantitation of the analytical methods. *Chron. Young Sci.* **2011**, *2*, 21–25. [CrossRef]
39. Miller, J.N.; Miller, J.C. *Statistics and Chemometrics for Analytical Chemistry*, 6th ed.; Pearson Education Ltd.: Harlow, UK, 2010.
40. Peltola, E.; Sainio, S.; Holt, K.B.; Palomäki, T.; Koskinen, J.; Laurila, T. Electrochemical Fouling of Dopamine and Recovery of Carbon Electrodes. *Anal. Chem.* **2018**, *90*, 1408–1416. [CrossRef]
41. Duvall, S.H.; McCreery, R.L. Self-Catalysis by Catechols and Quinones during Heterogeneous Electron Transfer at Carbon Electrodes. *J. Am. Chem. Soc.* **2000**, *122*, 6759–6764. [CrossRef]
42. Jackowska, K.; Krysinski, P. New Trends in the Electrochemical Sensing of Dopamine. *Anal. Bioanal. Chem.* **2013**, *405*, 3753–3771. [CrossRef] [PubMed]
43. Wang, D.; Pillier, F.; Cachet, H.; Debiemme-Chouvy, C. One-Pot Electrosynthesis of Ultrathin Overoxidized Poly(3,4-Ethylenedioxythiophene) Films. *Electrochim. Acta* **2022**, *401*, 139472. [CrossRef]
44. Pingarrón, J.M.; Yáñez-Sedeño, P.; González-Cortés, A. Gold Nanoparticle-Based Electrochemical Biosensors. *Electrochim. Acta* **2008**, *53*, 5848–5866. [CrossRef]
45. Lupu, S.; Lete, C.; Balaure, P.; Caval, D.; Mihailciuc, C.; Lakard, B.; Hihn, J.; Javier del Campo, F. Development of Amperometric Biosensors Based on Nanostructured Tyrosinase-Conducting Polymer Composite Electrodes. *Sensors* **2013**, *13*, 6759–6774. [CrossRef] [PubMed]
46. Anshori, I.; Kepakisa, K.; Rizalputri, L.; Althof, R.; Nugroho, A.; Siburian, R. Facile synthesis of graphene oxide/Fe_3O_4 nanocomposite for electrochemical sensing on determination of dopamine. *Nanocomposites* **2022**, *8*, 155–166. [CrossRef]
47. Roychoudhury, A.; Basu, S.; Kumar Jha, S. Dopamine biosensor based on surface functionalized nanostructured nickel oxide platform. *Biosens. Bioelectron.* **2016**, *84*, 72–81. [CrossRef]
48. Wasserstein, R.L.; Lazar, N.A. The ASA's Statement on p-Values: Context, Process, and Purpose. *Am. Stat.* **2016**, *70*, 129–133. [CrossRef]
49. Morgan, E. *Chemometrics: Experimental Design*, 1st ed.; John Wiley & Sons: Chichester, UK, 1995.